4200 J. Med. Chem. 2009, 52, 4200–4209
DOI: 10.1021/jm801399r

Journal of Medicinal Chemistry Article

Novel Lead Structures for p38 MAP Kinase via FieldScreen Virtual Screening

Timothy J. Cheeseright,[†] Melanie Holm,[‡] Frank Lehmann,[‡] Sabine Luik,[‡] Marcia Gottert,[‡] James L. Melville,[†] and Stefan Laufer*,[‡]

[†]*Cresset BioMolecular Discovery Ltd., BioPark Hertfordshire, Welwyn Garden City, Hertfordshire AL7 3AX, U.K., and* [‡]*Department of Pharmaceutical and Medicinal Chemistry, Institute of Pharmacy, Eberhard-Karls-University Tuebingen, Auf der Morgenstelle 8, D-72076 Tuebingen, Germany*

Received November 6, 2008

p38 MAP kinase has received considerable interest in the pharmaceutical industry and remains a valid and interesting target for the treatment of inflammation. To discover novel p38 inhibitors, we applied the ligand-based virtual screening technique, FieldScreen, to 1.2 million commercially available compounds. Fifty-eight diverse compounds were selected for biological analysis, using molecular field similarity to known inhibitors, while explicitly removing any structure that shared a scaffold with previously reported p38 inhibitors. Of these, 11 (19%) showed ≥20% inhibition of p38 at 10 μM. We chose to prepare analogues of two distinct chemical series resulting in a potential lead compound with pIC_{50} of 6.4. Modeling of SAR using FieldAlign, a ligand alignment protocol, was used to rationalize the SAR of the series of thiadiazole based inhibitors.

Introduction

Inflammation is a fundamental physiological process that is essential for survival but at the same time is one of the major causes of human morbidity and mortality. A large number of diseases have their seeds in the complex process of inflammation and specifically in an overactive immune response, the commonest of which include rheumatoid arthritis, psoriasis, multiple sclerosis, and inflammatory bowel diseases.[1]

The mitogen-activated protein kinase (MAPK[a]) p38 is one of the most extensively studied kinase target partly because of its important role as a key enzyme in the production of pro-inflammatory cytokines such as TNF-α and IL-1β. Of the four different isoforms of the p38 family (α, β, γ, and δ), p38α is ubiquitously expressed and is generally considered the most important isoform in the inflammatory signal transduction pathway and an appropriate target for anti-inflammatory therapy.

The initial discovery in 1994 of p38 as the molecular target for a novel class of cytokine suppressive inhibitors, exemplified by the prototypical inhibitor **1** (SB203580),[2] catalyzed the search for potent, selective, efficacious, and safe p38 inhibitors. These inhibitors show diversity not only in chemical structure but also in how they interact with the protein. To date, the well-known inhibitors can be divided into six classes (Figure 1): (1) pyridinyl- and pyrimidinylimidazoles and related structures, (2) bicyclic 6,6-heterocycles and related structures, (3) *N,N′*-diarylureas and related structures, (4) substituted benzamides, (5) diaryl ketones, and (6) indole amides.[3,4] However, few of these compounds have progressed beyond early stage clinical trials. Hence, there remains a great need for new lead structures for p38 MAPK.

Virtual screening is now an established method for hit finding within the pharmaceutical industry.[5] p38 inhibitors are popular choices for data sets for the retrospective validation of many virtual screening methods, including de novo design,[6] free energy calculations,[7] ligand-based similarity searching,[8] docking,[9] and QSAR.[10] Additionally, molecular dynamics[11] and docking[12] have been employed to rationalize the binding mode of known inhibitors. However, there are relatively few examples of the use of in silico methods for the *prospective* screening of p38 inhibitors. A notable example is provided by Jhoti and co-workers,[13] who used docking to construct target-specific fragment-based libraries, including one focused toward p38. Recently, FieldScreen,[14] a ligand-based similarity searching method using the concept of molecular fields,[15] has proven itself valuable for the task of scaffold hopping and virtual screening.[16] Therefore, we sought to apply this method for finding novel inhibitors of p38.

Design Process

As a similarity searching method, FieldScreen requires an active ligand to use as a search query, ideally in a bioactive conformation. We therefore reviewed the many ligands that have been cocrystallized with p38. We desired to mimic the closed form of the protein and hence immediately discounted ligands bound to alternative protein conformations. Of the remaining ligands, we gave preference to highly active druglike ligands and to ligands that occupied more of the active site. Using these criteria together with a visual inspection of the available ligands (ensuring that different chemotypes were chosen), we selected the ligands present in PDB codes 1m7q, 1yw2, and 1ouk. Each of the ligands present in these protein−ligand cocrystal structures was extracted and examined.

*To whom correspondence should be addressed. Phone: 0049-7071-2978788. Fax: 0049-7071-5961. E-mail: stefan.laufer@uni-tuebingen.de.

[a]Abbreviations: MAPK, mitogen-activated protein kinase; SAR, structure−activity relationship; FPP, field point pattern; ATF-2, activating transcription factor-2.

 Published on Web 06/02/2009 © 2009 American Chemical Society

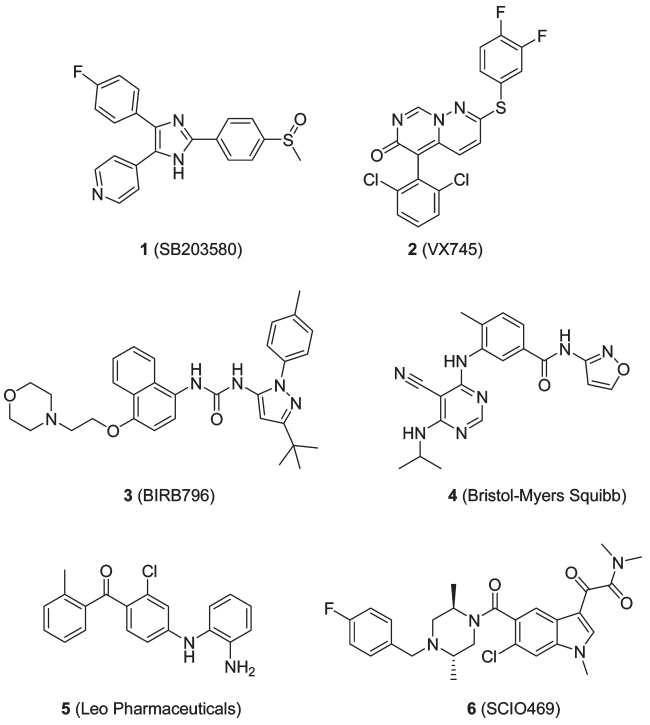

Figure 1. Overview of the different chemical classes of p38 inhibitors.

The ligand in PDB code 1m7q is a single digit nanomolar inhibitor of p38.[17] The ligand makes extensive contacts across the hinge region and into the specificity pocket. However, it also contains a piperazine moiety that is oriented toward the sugar and phosphate binding pockets. This group significantly changes the electrostatic field derived from the ligand, and so it was decided to truncate this part of the ligand to a simple dimethylamine (see Figure 2). This truncation promotes virtual screening hits that interact with the hinge binding region of p38 by increasing the proportion of the field descriptors derived from this important region relative to the size of whole field point pattern (FPP).

The ligand from PDB code 1yw2, like that from 1m7q, binds to a protein conformation where the backbone amide bond between Met^{109} and Gly^{110} is orientated to position the NH close to the ligand and available for H-bonding. In this respect both ligands present a strong negative field to the protein and consequently give large negative field points close to the carbonyl in 1m7q and the pyrimidine in 1yw2. However, the ligand from 1yw2 lacks the explicit N−H of 1m7q, presenting an aromatic hydrogen in its place giving a smaller positive field in the hinge region. The major feature of the 1yw2 ligand is the strong negative field points associated with the isoxalone moiety which interacts strongly with Lys^{53} in the protein ligand cocrystal, a feature that could be important in p38 inhibitors.

The final ligand that was chosen as a search query in our virtual screening strategy was that from PDB code 1ouk. In contrast to the other chosen inhibitors this ligand binds to a subtly different closed conformation of the protein. In the 1ouk protein−ligand cocrystal the amide bond between Met^{109} and Gly^{110} is oriented such that the carbonyl of Met^{109} is directed toward and interacts with the ligand. Consequently the field pattern of the ligand is more positive (as would be expected from an aminopyrimidine) and provides a good complement to the other selected search queries. In a similar manner to that described for the ligand of 1m7q, the highly polar piperidine was truncated to a methyl group to emphasize the hinge region over the sugar and phosphate binding pockets.

Taken together, the three chosen search queries present a diverse set of field point patterns to the protein. As such, it was envisaged that the three search queries would return markedly different hit lists.

In the processing of the results of the FieldScreen experiments it was decided to treat each of the three search queries identically and therefore to progress a fixed number of results from each hit list. Initially 250 results were taken from each result list with the intention of selecting 50−100 molecules for biological investigation. To aid the selection of molecules for purchase, the three hit lists were combined. Only four compounds were found to occur in more than one hit list. The remaining 746 compounds were clustered based on their 2D topologies. The resulting 96 clusters and 311 singletons were visually inspected in 2D and as 3D alignments relative to the original search query. In visually inspecting the 407 compounds, we applied the following criteria: reject if a similar scaffold was known as a p38 inhibitor; reject if the 3D alignment against the search query did not interact with the hinge region; reject if, in the opinion of our medicinal chemists, the database molecule appeared undruglike (e.g., excessive numbers of divalent sulfur atoms or nitro groups).

After visual inspection, 58 clusters were identified as potential p38 inhibitors. To accelerate biological analysis, it was decided to screen these clusters by choosing a representative molecule from each cluster. The molecule that was closest to the cluster center according to our 2D method was chosen for ordering and biological analysis.

Results

A selection of the compounds chosen for biological analysis is shown in Table 1 together with the inhibition obtained in an enzyme assay with ATF-2 as substrate and ATP as cosubstrate and with the inhibitor at a concentration of 10 μM.[18] Of the 58 compounds analyzed (the full list of compounds is given in the Supporting Information), 11 showed 20% or greater inhibition of p38 at 10 μM (a 19% hit rate). This was extremely encouraging given that we had specifically excluded compounds with obvious kinase binding motifs or that had been reported as p38 inhibitors previously.

To ensure that these results could not have been achieved using a simpler method, we used a 2D atom pairs similarity metric to screen the complete database of 1.2 million compounds against each of our three search queries.[19] For each of our search queries we constructed a results list consisting of the similarity rankings for each database molecule to the search query. By use of this method, the highest ranked compound of our chosen 58 was at positions 6600 (1yw2 based query), 20 400 (1m7q based query), and 26 300 (1ouk based query), well outside the top 250 we chose using FieldScreen.

We followed up the initial hits with a thorough patent and literature search around each scaffold. On the basis of this search and the initial activity that was found, we chose 3-(2-chlorophenyl)-6-((4-methoxyphenoxy)methyl)[1,2,4]triazolo[3,4-*b*][1,3,4]thiadiazole (**c15**) and 6-amino-1-benzyl-4-(4-bromophenyl)-3-methyl-1,4-dihydropyrano[2,3-*c*]pyrazole-5-carbonitrile (**c38**) for hit to lead investigations.

A small library of derivatives for the pyranopyrazole hit (**c38**) was prepared starting from different substituted pyrazol-5(4*H*)-ones.[20] Unfortunately this library showed only

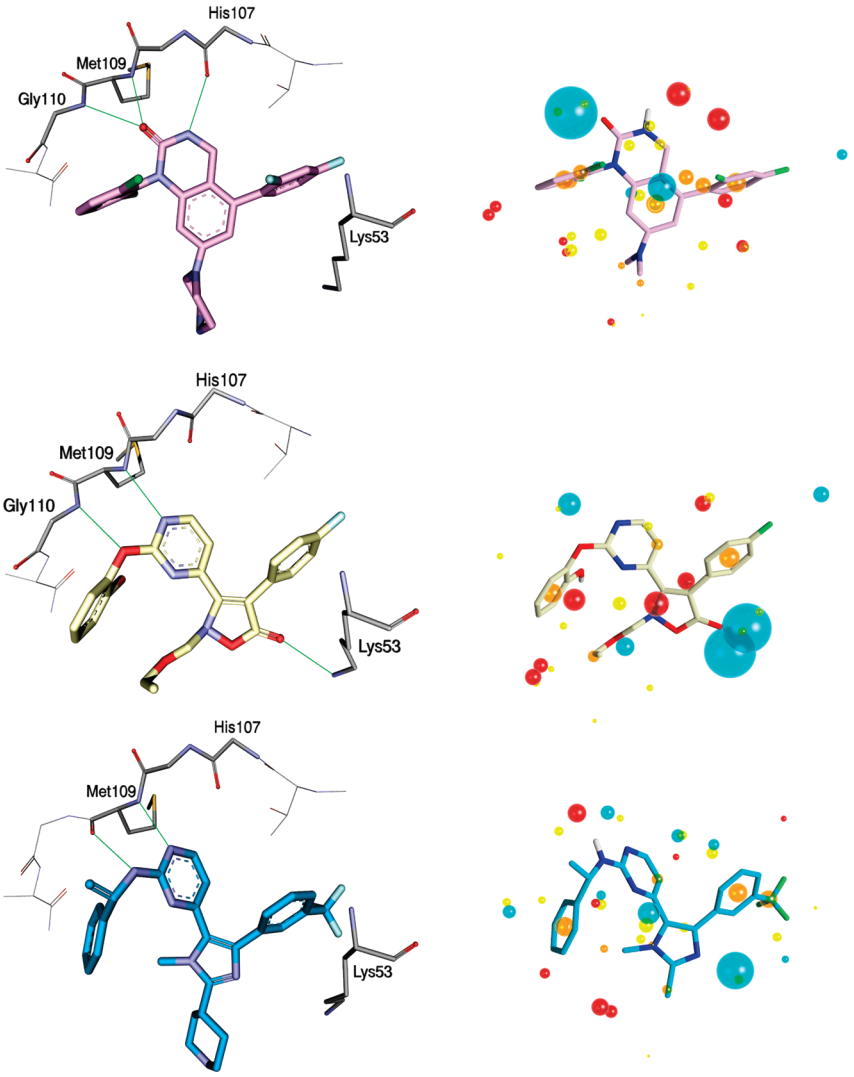

Figure 2. Ligands from PDB codes 1m7q (top), 1yw2 (middle), 1ouk (bottom): ligand as present in PDB file showing selected protein residues and H-bonds (green lines); ligand used as search query including field point patterns. Key to field point colors are as follows: blue = negative; red = positive; orange = hydrophobic; yellow = surface.

moderate SAR across more than 20 analogues, and hence, our attention turned to the thiadiazole series.

We pursued SAR of **c15** through a strategy of purchase and synthesis. Where useful analogues were commercially available we purchased them (Figure 1 in Supporting Information). However, not all the analogues that we wished to screen were commercially available, and hence, we embarked on a synthesis of key analogues. The synthesis of derivatives of **c15** was achieved by preparing a range of triazole intermediates that were reacted with carboxylic acids in refluxing phosphorus oxychloride.[21] The triazole intermediates were prepared directly from appropriate carboxylic acids by warming a mixture with thiocarbohydrazide to the melting temperature.[22] Where this approach was unsuccessful the triazole was formed by reacting suitable carboxylic acids with hydrazine and treating the resulting hydrazides with carbon disulfide (Scheme 1) followed by a further reaction with hydrazine to furnish the desired triazole intermediate.[23]

Thirty-two 3,6-disubstituted [1,2,4]triazolo[3,4-*b*][1,3,4]-thiadiazoles were tested with inhibitions up to 83% (IC_{50} = 0.44 μM) (Table 2 and Supporting Information Figure 1) and distinct SAR can be summarized as follows (Figure 3). Essential for inhibitory activity is a bulky lipophilic residue in the 3-position. Incorporation of an *o*-substituted phenyl residue gave significant and consistent increase in inhibition, suggesting that a twisted conformation is strongly preferred in this region.

Structural change to *m*-, *p*-substitution or two residues in *o*- and *p*-position gave a reduction in potency as did extending from a phenyl to a benzyl substituent. In the same way, a switch to a furyl residue or other five- and six-membered heterocycles, respectively, resulted in loss of inhibition potency. Substitution in the 6 position gave significant changes in activity. Moving the para methoxy substituent to the meta position led to a sharp drop in activity, whereas removal of the *p*-methoxy substiuent of **c15** led to a small increase in activity. Swapping the ether linker to the equivalent alkane gave little change in activity, whereas truncation of the *p*-methoxylphenoxymethyl substituent to a *p*-methoxybenzyl group led to a gain in activity.

To further understand our SAR, we chose to carry out a field-based alignment of the thiadiazole analogues to our original search queries, using the program FieldAlign. In this procedure the three search queries were loaded into FieldAlign as a single reference molecule. Next, each member of the pyrazole series was conformationally explored and each conformation of each molecule was aligned to the combined

Table 1. Inhibitors Discovered by Screening

structure	% [a,b]	structure	% [a,b]	structure	% [a,b]
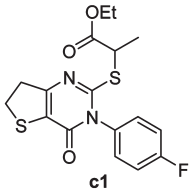 **c1**	23±0.81	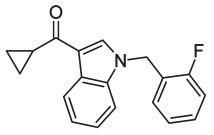 **c27**	23±4.35	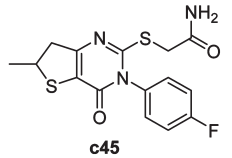 **c45**	4±2.11
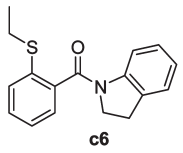 **c6**	4±3.05	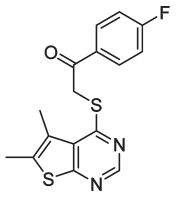 **c32**	24±1.38	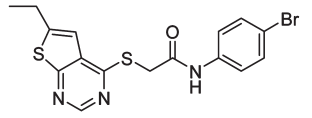 **c47**	14±1.23
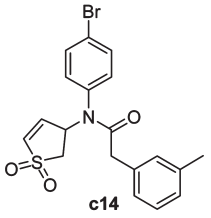 **c14**	2±2.18	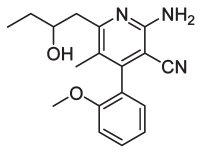 **c33**	20±6.40	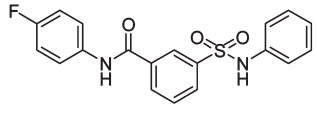 **c50**	15±8.35
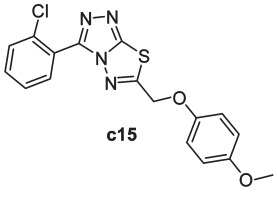 **c15**	68±0.99	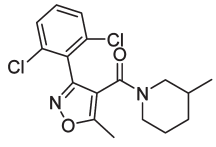 **c35**	14±7.27	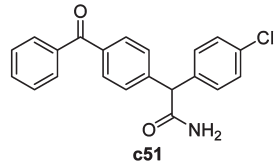 **c51**	26±3.10
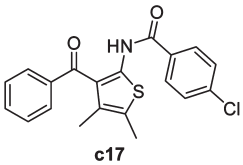 **c17**	31±1.98	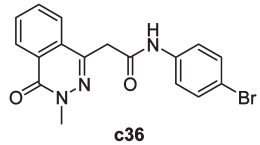 **c36**	15±3.45	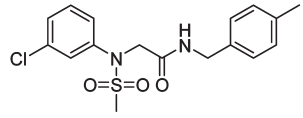 **c52**	1±0.68
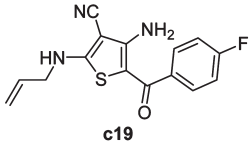 **c19**	46±3.09	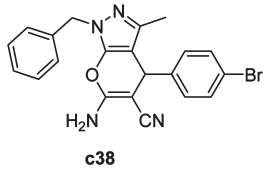 **c38**	40±2.09	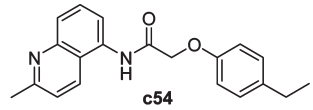 **c54**	4±2.56
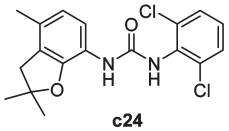 **c24**	66±0.81	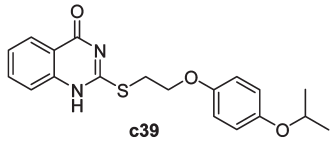 **c39**	23±2.10	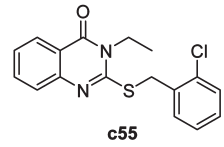 **c55**	28±3.58
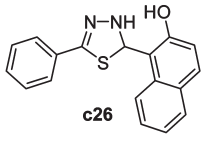 **c26**	21±10.9	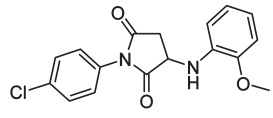 **c44**	20±1.97	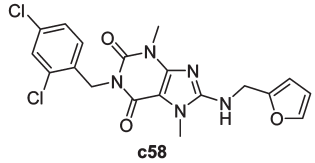 **c58**	-

[a] Inhibition at 10 μM. [b] Number of determinations was 3.

reference. For an alignment to score well, the conformation under study must align well to each component of the reference molecule in a single orientation. Using a multiple molecule reference in this manner gives a better description of the requirements of the protein for the binding of ligands. Gratifyingly a single, consistent binding mode was suggested by these experiments (Figure 4). Our modeling suggested that the R_1 substituent binds to the hydrophobic pocket close to Met^{109} and Gly^{110}, the nitrogens of the diazole interact with the hinge region, and the R_2 substituent occupies the kinase selectivity pocket (Figure 4). This binding mode is consistent with the observed SAR.

Scheme 1. Synthesis of 3,6-Disubstituted Triazolo[3,4-*b*][1,3,4] thiadiazoles (**17**−**48**)[a]

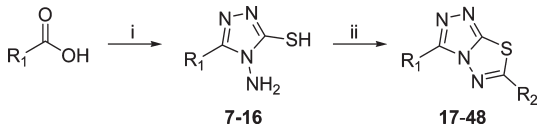

7-16 **17-48**

[a] Reagents and conditions: (i) thiocarbohydrazide, "ball-tube oven" ("Kugelrohr apparatus"), melting temp or (1) H_2SO_4, EtOH, 8 h, reflux, (2) N_2H_4, ethanol, 6 h, reflux, (3) CS_2, EtOH, 12 h, room temp, (4) N_2H_4, MeOH, 6 h, room temp; (ii) R_2-COOH, $POCl_3$, 6 h, reflux.

Conclusion

p38 MAP kinase remains a valid and interesting target for therapeutic intervention in inflammatory diseases. Using a novel ligand based virtual screening method, we searched commercially available compounds for novel actives. The crude results list was found to be rich in chemotypes that were known to be inhibitors of p38, validating the choice of search queries and the search method. However, the known chemotypes were now removed from the hit list before further selection of compounds to purchase. From this new list we chose just 58 compounds for biological analysis, representing just 0.003% of the 1.2 million compounds originally searched. Pleasingly, we found an excellent hit rate even among this highly selected data set. This surprisingly positive result served to justify our choice of a ligand based method in this project where conventional practice would have employed a structure based approach. Furthermore, there have been few examples of molecular field based technologies being used in virtual screening in either a retrospective or prospective manner. A recent communication on the application of FieldScreen to a retrospective data set suggested that it would perform poorly for p38 kinase.[14] Clearly the results of this application of FieldScreen are above expectations.

We chose to follow up compounds found to be active in biological analysis with a dual strategy of purchase and synthesis. Compound purchase was very attractive, as it provided rapid SAR, but it proved difficult to get a full set of rationally designed compounds. For this reason we also chose, and have described here, the synthesis of small libraries of compounds around two of the most active hits. Additionally, field based alignment of analogues was used to facilitate the interpretation of our biological data and enabled us to propose a binding mode for one of these series. We anticipate that the binding models will greatly aid our future elaboration of the 3,6-disubstituted triazolo[3,4-*b*][1,3,4]thiadiazoles series.

Experimental Section

FieldScreen Virtual Screening. Field-based 3D similarity searching was carried out using FieldScreen.[14] In FieldScreen, each molecule is described as a Field Point Pattern (FPP),[15] using the local extrema of four molecular fields: positive electrostatic, negative electrostatic, surface (van der Waals interactions), and hydrophobic. The resulting FPPs are aligned and scored to give a measure of similarity between a query molecule and a database molecule in specific conformations. For the query molecule, conformations were taken from the coordinates of the X-ray structures. For the database molecules, 50 conformations were generated per molecule using the XedeX[25] conformation hunter, and each conformation was scored separately to the query molecule. The similarity of the best scoring conformation for each database molecule was reported. The comparison of field point patterns can be performed at three levels of accuracy: FieldPrint, FieldClique, and FieldSimplex. In a FieldPrint comparison, each pair of field points in a molecule is recorded, along with the distance, type, and the intensity of their interaction (represented as the product of the size of the field points). The distances are binned (with a spacing of 1.5 Å), and the most intense interaction of a given type and distance range is stored. This produces a field "fingerprint" for each molecule, which is used to compare two molecules without requiring an alignment step. The top 40% scoring molecules were carried through to FieldClique screening. FieldClique comparisons identify sets of field points that are common to both molecules via a clique perception algorithm. These field points are then used to align the two molecules. The alignment is scored by sampling the field of the query conformation at the positions defined by the field points of the database conformation. This process is then reversed so that the field of the database conformation is sampled by the field points of the query conformation. The extents to which the field points of one conformation sample a similar field in the other conformation are combined to produce the final similarity value for the two conformations. The final stage in the FieldScreen process was to optimize the alignment of the top scoring molecules from FieldClique using a multidimensional simplex minimization of the rigid conformations.[15] This FieldSimplex routine gives the most accurate measure of field similarity for any molecule within the FieldScreen system. Additionally, an excluded volume can be defined surrounding a search query such that any atom in any alignment that enters the excluded volume causes a penalty to be added to the scoring function. The excluded volume was defined using the conformation of the protein in the appropriate protein−ligand crystal structure. The resulting hit list was clustered with the group average linkage method,[26] using topological atom pairs as descriptors,[19,27] and a Dice similarity coefficient threshold of 0.7 for merging two clusters.

Ligand preparation was performed by alignment and superposition of the proteins in PDB codes 1m7q, 1ouk, and 1yw2 (manual alignment of equivalent residues, superposition of equivalent C-α atoms using Accelrys DS Visualizer 1.6) followed by correction of the bonding pattern of each of the ligands. Analysis of each protein ligand crystal structure led to the truncation of the ligands present in structures 1m7q and 1ouk as described above. Finally the modified ligands were exported for use in FieldScreen in sdf format.

Molecular Alignment. Field based 3D molecular alignment was carried out using FieldAlign, version 2.0.1,[28] in an analogous manner to that described for the FieldSimplex routine of FieldScreen above. However, multiple prealigned single conformations were used as the reference in the alignment. The reference was constructed by importing each of the ligands that were prepared as FieldScreen search queries into a single FieldAlign project. Molecules to be aligned (database molecules) were either pasted directly from a relevant drawing package or read in from an sdf file. Each database molecule was conformationally explored within FieldAlign (keeping a maximum of 100 conformations) before the addition of molecular field points and alignment to the multimolecule template. FieldAlign returns the best alignment based on the mean of the scores to the individual members of the reference in a given orientation.

Biological Testing. According to the developed method,[18] test compounds were tested in concentrations ranging from 10^{-5} to 10^{-8} M. Pyridinylimidazole **1** was used as a reference compound, and the optimized ATP concentration at which the test was performed was 100 μM. Briefly the assay involves the immobilization of the kinase substrate ATF-2 (activating transcription factor-2) on microtiter plates, addition of the kinase reaction mixture, and measurement of substrate phosphorylation using a two-step antigen−antibody reaction in which the primary antibody binds to the double (Thr69 and Thr71) phosphorylated ATF-2 and acts as antigen for the secondary antibody. Secondary antibody is conjugated with alkaline phosphatase which is able,

Table 2. Biological Activity of Synthesized 3,6-Disubstituted Triazolo[3,4-*b*][1,3,4]thiadiazoles[c]

cmpd	structure	%[a,b]	IC_{50} ±SEM[μM][b]
p15	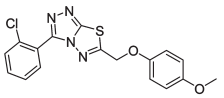	68±0.99	
17	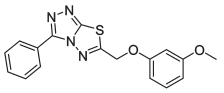	11±4.62	-
18	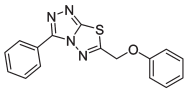	39±3.04	-
19	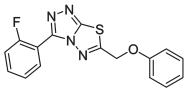	73±1.83	3.08±0.47
20	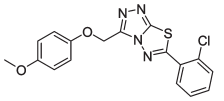	34±0.38	-
21	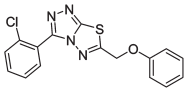	76±0.73	0.79±0.06
22	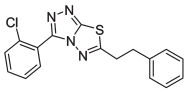	72±1.05	2.55±0.17
23	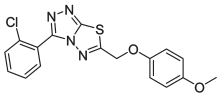	64±3.30	3.88±0.89
24	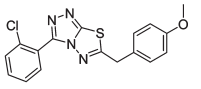	83±0.64	0.44±0.17
25	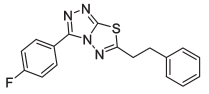	32±3.77	-
26	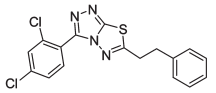	45±2.25	-
27	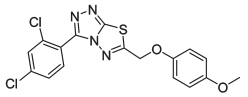	31±2.40	-
28	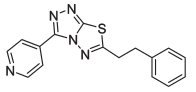	26±1.52	-
29*	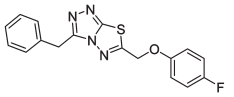	32±3.02	-
30*	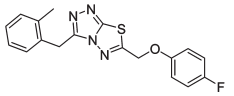	36±2.02	-
31*	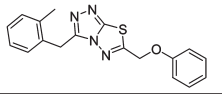	33±0.84	-
32*	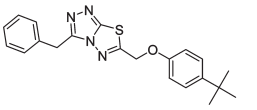	12±4.01	-
33*	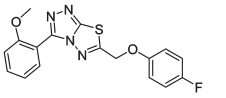	79±0.82	0.65±0.12
34*	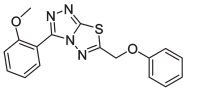	77±3.08	0.74±0.01
35*	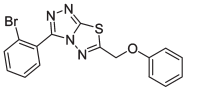	80±4.66	1.24±0.35
36*	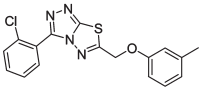	76±0.66	1.98±0.16
37*	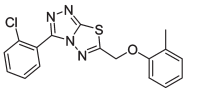	65±5.36	3.51±1.13
38*	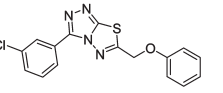	3±1.88	-
39*	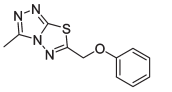	18±1.58	-
40*	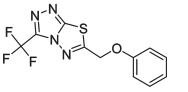	16±2.10	-
41*	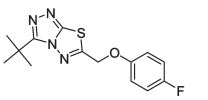	53±1.85	4.71±0.40
42*	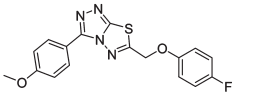	31±2.01	-
43*	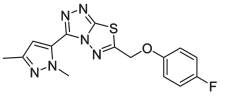	22±4.06	-
44*	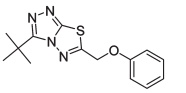	61±0.52	3.98±1.27
45*	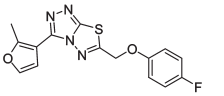	21±2.06	-
46*	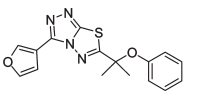	24±2.99	-
47*	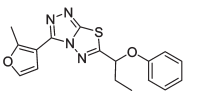	31±1.31	-
48*	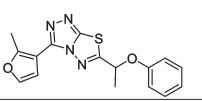	30±4.00	-

[a] Inhibition at 10 μM. [b] Number of determinations was 3. [c] The asterisk (∗) indicates purchased 3,6-disubstituted [1,2,4]triazolo[3,4-*b*][1,3,4]-thiadiazoles.

in the last step, to dephosphorylate 4-nitrophenolphosphate disodium salt (4-NPP), 4-nitrophenol being the detected species by an ELISA reader at 405 nm.

Chemistry. Infrared spectra were recorded on a "Perkin-Elmer Spectrum One" infrared spectrophotometer. ^{1}H (200 MHz, digital resolution 0.3768 Hz) and ^{13}C (50 MHz, digital resolution 1.1299 Hz) NMR data were recorded on a Bruker AC 200. The data are reported as follows: chemical shift in ppm from Me_4Si as external standard, multiplicity, and coupling constant (Hz). GC−MS was performed on a HP6890 series system. EI mass spectra were recorded on a Varian MAT 311A (70 eV) and FD mass spectra on a MAT-95 (Finnigan). LC/MS (ESI) was performed on a Thermo Finnigan Surveryer system with Thermo Finnigan TSQ Quantum triple quadrupole mass spectrometer. HPLC was carried out on Merck Hitachi L-6200A intelligent pump, Merck Hitachi AS-2000A autosampler, and Merck Hitachi L-4250 UV−vis detector. HRMS (EI) (electron impact high resolution mass spectrometry) was executed at the Abteilung fur Massenspektrometrie des Instituts fur Organische Chemie der Universitat Tubingen. For clarity, only the highest measured signal is given for FD mass spectra. Buchi melting point B-545 apparatus was used, and melting points are uncorrected. Where appropriate, column chromatography was performed for crude precursors with Merck silica gel 60 (0.063−0.200 mm). Column chromatography for test compounds was performed using a La-Flash system (VWR) with Merck silica gel 60 (0.015−0.040 mm) or RP18 columns. The progress of the reactions was monitored by thin-layer chromatography (TLC) performed with Merck silica gel 60 F-245 plates. Where necessary, reactions were carried out in a nitrogen atmosphere using 4 Å molecular sieves. All reagents and solvents were obtained from commercial sources and used as received. Reagents were purchased from Sigma-Aldrich Chemie, Steinheim, Germany; from VWR, Darmstadt, Germany; or from Acros, Geel, Belgium. The *β*-keto esters, 1*H*-pyrazol-5(4*H*)-ones, and dihydropyrano[2,3-*c*]pyrazoles (**1**−**30**) were recently published.[20]

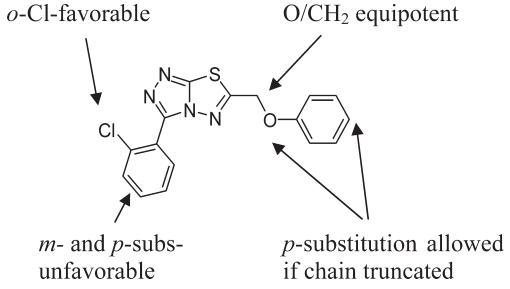

Figure 3. Analysis of SAR for thiadiazole series.

General Method A for 5-Substituted [1,2,4]Triazoles. Equimolar amounts of the appropriate acid and thiocarbohydrazide were carefully heated up to the melting point (160−180 °C) in a "ball-tube oven" ("Kugelrohr apparatus") under slow rotation until the liquefied material got solid again (20−30 min). The solidified smelter was dissolved in the required amount of ethanol and optionally up-concentrated until the product precipitated.

4-Amino-5-phenyl-4*H*-1,2,4-triazole-3-thiol (7). Yield: 61%. ^{1}H NMR (200 MHz, DMSO-d_6): δ [ppm] = 5.80 (s, 2H, $-NH_2$), 7.51−8.17 (m, 5H, 2′,3′,4′,5′,6′-H), 13.93 (s, 1H, −SH). GC−MS (EI): 10.16 min, *m*/*z* [%] = 193.0 (12), 192.0 ([M*], 100), 121.0 (20), 104.0 (23), 77.0 (18). IR: 3072 (w), 2832 (w), 2666 (w), 2555 (w), 1680 (s), 1601 (m), 1583 (m), 1535 (w), 1497 (w), 1453 (m), 1421 (m), 1324 (m), 1289 (s), 1186 (m), 1128 (m), 1101 (w), 1073 (m), 1027 (m), 1000 (w), 932 (s), 805 (m), 704 (s), 684 (m), 667 (s). Mp: 227.1 °C.

4-Amino-5-(2-fluorophenyl)-4*H*-1,2,4-triazole-3-thiol (8). Yield: 58%. ^{1}H NMR (200 MHz, DMSO-d_6): δ [ppm] = 5.64 (s, 2H, $-NH_2$), 7.51−7.99 (m, 5H, 2′,3′,4′,5′,6′-H), 14.03 (s, 1H, −SH). GC−MS (EI): 11.93 min, *m*/*z* [%] = 211.0 (12), 210.0 ([M*], 100), 139.0 (28), 122.0 (28), 121.0 (25), 95.0 (16), 60.0 (11). IR: 3310 (w), 1625 (w), 1451 (m), 1318 (w), 1237 (m), 1055 (w), 1003 (w), 950 (m), 822 (m), 765 (s), 726 (m), 681 (m), 629 (m), 602 (m), 535 (m), 476 (w), 440 (w). Mp: 181.6 °C.

4-Amino-5-benzyl-4*H*-1,2,4-triazole-3-thiol (9). Yield: 67%. ^{1}H NMR (200 MHz, DMSO-d_6): δ [ppm] = 4.02 (s, 2H, $-CH_2-$), 5.80 (s, 2H, $-NH_2$), 7.32−7.23 (m, 5H, 2′,3′,4′,5′,6′-H), 13.53

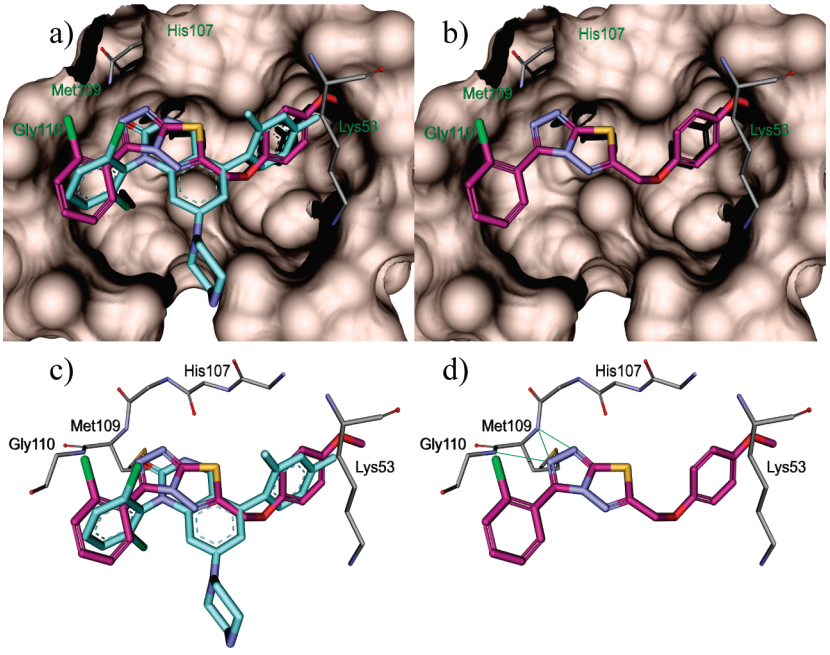

Figure 4. Proposed binding mode of the thiadiazole series, obtained by 3D molecular alignment of compound **c15** to the three prealigned ligands of PDB codes 1m7q, 1ouk, and 1yw2. Shown are selected residues from 1m7q and compound **c15** (magenta) and in (a) the native ligand of 1m7q (cyan), (c) modeled orientation of compound **c15** in the active site of p38 from PDB code 1m7q relative to the native ligand (d) showing potential H-bond interactions to the hinge region.[15] (a) and (b) show a solvent accessible surface of protein 1m7q as calculated in DS Visualizer 2.0 using a probe radius of 1.4.[24]

(s, 1H, −SH). GC−MS (EI): 13.35 min, *m*/*z* [%] = 207.1 (13), 206.1 ([M*], 100), 190.0 (17), 117.1 (10), 93.1 (11), 91.1 (36).

4-Amino-5-(2-chlorobenzyl)-4*H*-1,2,4-triazole-3-thiol (10). Yield: 66%. ^{1}H NMR (200 MHz, DMSO-d_6): δ [ppm] = 4.13 (s, 2H, $-CH_2-$), 5.59 (s, 2H, $-NH_2$), 7.20−7.55 (m, 5H, 2′,3′,4′,5′,6′-H), 13.53 (s, 1H, −SH). GC−MS (EI): 13.04 min, *m*/*z* [%] = 242.1 (32), 241.1 (10), 240.1 ([M*], 79), 205.1 (54), 188.1 (63), 127.0 (40), 126.0 (11), 125.0 (100), 116.1 (48), 89.1 (82), 63.1 (43), 60.0 (71), 59.0 (49). IR: 3147 (w), 1594 (w), 1475 (m), 1419 (m), 1306 (m), 1054 (m), 1037 (m), 1012 (m), 979 (m), 838 (w), 802 (w), 813 (s), 751 (s), 682 (m), 662 (m), 641 (m), 554 (m), 464 (w), 445 (w). Mp: 204.8 °C.

4-Amino-5-phenethyl-4*H*-1,2,4-triazole-3-thiol (11). Yield: 63%. ^{1}H NMR (200 MHz, DMSO-d_6): δ [ppm] = 2.94 (s, 4H, $-CH_2-CH_2-$), 5.61 (s, 2H, $-NH_2$), 7.13−7.35 (m, 5H, 4′,5′,6′,7′,8′-H), 13.44 (s, 1H, −SH). GC−MS (EI): 12.75 min, *m*/*z* [%] = 221.0 (14), 220.0 ([M*], 100), 91.0 (100), 65.1 (16), 60.0 (10). IR: 3140 (w), 2933 (w), 1636 (w), 1571 (m), 1481 (m), 1420 (m), 1309 (m), 1146 (w), 1090 (w), 1045 (m), 971 (m), 748 (s), 699 (s), 655 (m), 580 (m), 531 (m), 498 (m), 473 (m). Mp: 227.9 °C.

4-Amino-5-((4-methoxyphenoxy)methyl)-4*H*-1,2,4-triazole-3-thiol (12). Yield: 62%. ^{1}H NMR (200 MHz, DMSO-d_6): δ [ppm] = 3.70 (s, 3H, $-CH_3$), 5.04 (s, 2H, $-CH_2-$), 5.69 (s, 2H, $-NH_2$), 6.84−6.89 (d, 2H, ^3J = 9.16 Hz, 2′,6′-H), 6.96−7.01 (d, 2H, ^3J = 9.16 Hz, 3′,5′-H),13.79 (s, 1H, −SH). GC−MS (EI): 14.35 min, *m*/*z* [%] = 252.0 ([M*], 26), 124.0 (100), 123.0 (52), 109.0 (30), 95.0 (22), 81.0 (12). IR: 3142 (w), 2031 (w), 1580 (w), 1503 (m), 1462 (w), 1286 (w), 1223 (m), 1082 (w), 1031 (m), 982 (w), 812 (m), 735 (s), 665 (m), 607 (w), 514 (m), 482 (m). Mp: 176.8 °C.

General Method B for 5-Substituted [1,2,4]Triazoles. Carbon disulfide (3.3 mL, 5.5 mmol) was added dropwise to a solution of the suitable hydrazide (3.6 mmol) in ethanol (70 mL) containing potassium hydroxide (3.0 g, 5.5 mmol). The mixture was stirred at room temperature overnight, then cooled with an ice bath and diluted with diethyl ether. The precipitate was filtered, washed with diethyl ether, and dried. The hydrazinecarbodithioates were obtained in quantitative yields and used without further purification.

Hydrazine hydrate (2.4 mmol) was added to a solution of the potassium salt (1.6 mmol) suspended in water (2 mL), and the mixture was refluxed under stirring for 6 h. To the cooled reaction mixture, water (80 mL) was added and the solution acidified with concentrated hydrochloric acid. The precipitate was filtered with water and dried.

4-Amino-5-(4-fluorophenyl)-4*H*-1,2,4-triazole-3-thiol (13). Yield: 75%. ^{1}H NMR (200 MHz, DMSO-d_6): δ [ppm] = 5.78 (s, 2H, $-NH_2$), 7.33−8.12 (m, 4H, 2′,3′,5′,6′-H), 13.89 (s, 1H, −SH). GC−MS (EI): 11.92 min, *m*/*z* [%] = 211.0 (12), 210.0 ([M*] 100), 139.0 (28), 122.0 (28), 121.0 (25), 95.0 (16), 60.0 (11).

4-Amino-5-(2-chlorophenyl)-4*H*-1,2,4-triazole-3-thiol (14). Yield: 77%. ^{1}H NMR (200 MHz, DMSO-d_6): δ [ppm] = 5.59 (s, 2H, $-NH_2$), 7.54−7.68 (m, 4H, 3′,4′,5′,6′-H), 13.99 (s, 1H, −SH). GC−MS (EI): 12.38 min, *m*/*z* [%] = 227.0 (12), 226.0 ([M*], 100), 158.0 (11), 154.9 (23), 140.0 (10), 138.0 (30), 102.0 (32), 75.0 (16), 60.0 (19). IR: 3083 (w), 1629 (w), 1556 (w), 1488 (m), 1460 (m), 1327 (m), 1128 (w), 1080 (w), 1047 (m), 997 (m), 938 (s), 766 (s), 733 (m), 759 (s), 602 (s), 534 (w), 463 (m), 417 (w). Mp: 161.8 °C.

4-Amino-5-(2,4-dichlorophenyl)-4*H*-1,2,4-triazole-3-thiol (15). Yield: 81%. ^{1}H NMR (200 MHz, DMSO-d_6): δ [ppm] = 5.78 (s, 2H, $-NH_2$), 7.60−7.88 (m, 3H, 3′,5′,6′-H), 14.06 (s, 1H, −SH). GC−MS (EI): 13.55 min, *m*/*z* [%] = 263.9 (15), 261.9 (73), 261.0 (13), 259.9 ([M*], 100), 190.9 (20), 188.9 (30), 173.9 (18), 172.9 (19), 171.9 (28), 170.9 (27), 136.0 (22), 100.0 (17), 60.0 (20). IR: 3093 (w), 1602 (w), 1563 (w), 1487 (m), 1374 (w), 1334 (m), 1147 (w), 1100 (m), 1045 (w), 949 (m), 864 (m), 843 (m), 813 (s), 734 (m), 624 (m), 569 (w), 525 (w), 479 (m), 436 (w). Mp: 213.6 °C.

4-Amino-5-(pyridin-4-yl)-4*H*-1,2,4-triazole-3-thiol (16). Yield: 72%. ^{1}H NMR (200 MHz, DMSO-d_6): δ [ppm] = 5.86 (s, 2H, $-NH_2$), 8.00−8.03 (d, 2H, ^3J = 6.13 Hz, 2′,6′-H), 8.74−8.77 (d, 2H, ^3J = 6.13 Hz, 3′,5′-H), 13.89 (s, 1H, −SH). IR: 3158 (w), 2450 (w), 1812 (w), 1606 (m), 1572 (w), 1517 (w), 1449 (w), 1415 (w), 1315 (m), 1217 (w), 1086 (w), 1064 (w), 1038 (w), 1004 (m), 941 (s), 824 (s), 736 (w), 709 (w), 688 (m), 6001 (s), 528 (m), 498 (m). Mp: 235.4 °C.

General Method for 3,6-Disubstituted [1,2,4]Triazolo[3,4-*b*][1,3,4]thiadiazoles. A mixture of the selected triazole (1.00 equiv), the corresponding carboxylic acid (2.00 equiv), and phosphorus oxychloride (22.0 equiv) was refluxed for about 6 h. The reaction mixture was poured on crushed ice. The solid thus separated was filtered and treated with NaOH solution (aqueous 10%) to remove the unreacted material. The solid residue was filtered, washed with water, and crystallized from ethanol.

6-((3-Methoxyphenoxy)methyl)-3-phenyl[1,2,4]triazolo[3,4-*b*][1,3,4]thiadiazole (17). Yield: 74%. ^{1}H NMR (200 MHz, DMSO-d_6): δ [ppm] = 3.76 (s, 3H, $-CH_3$), 5.62 (s, 2H, $-CH_2-$), 6.72−7.21 (m, 4H, 4″,5″,6″,8″-H), 7.64 −8.25 (m, 5H, 2′,3′,4′,5′,6′-H). IR: 1589 (w), 1478 (m), 1466 (m), 1376 (w), 1229 (m), 1170 (w), 1079 (w), 1055 (w), 1014 (w), 968 (m), 827 (w), 801 (w), 751 (s), 728 (m), 690 (m), 663 (m), 554 (w), 507 (m), 464 (m), 434 (w). Mp: 136.7 °C. HPLC purity: 99.9% (t_R = 6.77 min).

6-(Phenoxymethyl)-3-phenyl[1,2,4]triazolo[3,4-*b*][1,3,4]thiadiazole (18). Yield: 70%. ^{1}H NMR (200 MHz, DMSO-d_6): δ [ppm] = 5.43 (s, 2H, $-CH_2-$), 7.35−7.62 (m, 5H, 4″,5″,6″,7″,8″-H), 8.32 −8.39 (m, 5H, 2′,3′,4′,5′,6′-H). IR: 2980 (w), 1587 (w), 1468 (m), 1364 (w), 1294 (w), 1238 (m), 1171 (m), 1079 (w), 1053 (m), 1016 (w), 967 (m), 823 (w), 771 (w), 756 (s), 684 (s), 511 (m). Mp: 146.0 °C. HPLC purity: 99.4% (t_R = 7.55 min). HRMS: calcd for $C_{16}H_{12}N_4OS$ [$M^{\bullet+}$] 308.0732, found 308.0749.

3-(2-Fluorophenyl)-6-(phenoxymethyl)[1,2,4]triazolo[3,4-*b*][1,3,4]thiadiazole (19). Yield: 71%. ^{1}H NMR (200 MHz, DMSO-d_6): δ [ppm] = 5.58 (s, 2H, $-CH_2-O-$), 7.58−8.09 (m, 9H, 2′,3′,4′,5′,4″,5″,6″,7″,8″-H). IR: 1589 (w), 1467 (m), 1376 (w), 1230 (m), 1122 (w), 1079 (w), 1055 (w), 1014 (w), 969 (m), 827 (w), 800 (w), 751 (s), 728 (m), 690 (m), 663 (m), 555 (w), 507 (m), 464 (m), 434 (m). Mp: 140.1 °C. HPLC purity: 99.9% (t_R = 7.08 min). HRMS: calcd for $C_{17}H_{13}ClN_4O_2S$ [$M^{\bullet+}$] 326.0637, found 326.0622.

6-(2-Chlorophenyl)-3-((4-methoxyphenoxy)methyl)[1,2,4]triazolo[3,4-*b*][1,3,4]thiadiazole (20). Yield: 74%. ^{1}H NMR (200 MHz, DMSO-d_6): δ [ppm] = 3.70 (s, 3H, $-OCH_3$), 5.50 (s, 2H, $-CH_2-$), 6.85−6.90 (d, 2H, ^3J = 9.22 Hz, 4′,8′-H), 7.03−7.07 (d, 2H, ^3J = 9.22 Hz, 5′,7′-H), 7.54−8.04 (m, 4H, 3″,4″,5″,6″-H). IR: 2980 (w), 1594 (w), 1502 (m), 1447 (m), 1356 (w), 1304 (w), 1231 (s), 1106 (m), 1019 (m), 820 (s), 761 (m), 718 (s). Mp: 145.9 °C. HPLC purity: 99.9% (t_R = 7.01 min).

3-(2-Chlorophenyl)-6-(phenoxymethyl)[1,2,4]triazolo[3,4-*b*][1,3,4]thiadiazole (21). Yield: 77%. ^{1}H NMR (200 MHz, DMSO-d_6): δ [ppm] = 5.56 (s, 2H, $-CH_2-$), 6.99−8.03 (m, 9H, 3′,4′,5′,6′,4″,5″, 6″,7″,8″-H). IR: 2916 (w), 1590 (w), 1488 (w), 1467 (m), 1365 (w), 1229 (m), 1170 (w), 1081 (w), 1051 (m), 970 (m), 817 (w), 725 (s), 690 (m), 511 (w). Mp: 127.4 °C. HPLC purity: 99.9% (t_R = 7.13 min). HRMS: calcd for $C_{16}H_{11}ClN_4OS$ [$M^{\bullet+}$] 342.0342, found 342.0335.

3-(2-Chlorophenyl)-6-phenethyl[1,2,4]triazolo[3,4-*b*][1,3,4]thiadiazole (22). Yield: 72%. ^{1}H NMR (200 MHz, DMSO-d_6): δ [ppm] = 3.06 (t, 2H, ^3J = 7.58 Hz, 1″-H), 3.39 (t, 2H, ^3J = 7.96 Hz, 2″-H), 7.15−7.76 (m, 9H, 3′,4′,5′,6′,4″,5″,6″,7″,8″-H). GC−MS (EI): 13.43 min, *m*/*z* [%] = 342.10 (38), 341.10 (21), 340.10 ([M*] (96), 139.00 (10), 137.00 (27), 115.10 (10), 102.00 (15), 91.10 (100). IR: 3001 (w), 1526 (w), 1496 (w), 1453 (s), 1137 (w), 1229 (m), 1106 (w), 1078 (w), 1052 (w), 1005 (w), 967 (m), 845 (w), 754 (s), 732 (m), 720 (s), 700 (s), 657 (m), 639 (m), 534 (m), 480 (m), 456 (w). Mp: 160.1 °C. HPLC purity: 99.9% (t_R = 7.33 min). HRMS: calcd for $C_{17}H_{13}ClN_4S$ [$M.^+$] 340.0549, found 340.0530.

3-(2-Chlorophenyl)-6-((4-methoxyphenoxy)methyl)[1,2,4]triazolo[3,4-*b*][1,3,4]thiadiazole (23). Yield: 75%. ^{1}H NMR

(200 MHz, DMSO-d_6): δ [ppm] = 3.70 (s, 3H, $-CH_3$), 5.49 (s, 2H, $-CH_2-$), 7.15−7.76 (m, 9H, 3′,4′,5′,6′,4″,5″,6″,7″,8″-H). IR: 2837 (w), 1596 (w), 1555 (w), 1506 (s), 1465 (m), 1444 (m), 1352 (w), 1308 (w), 1234 (s), 1184 (m), 1106 (w), 1052 (m), 1032 (m), 961 (m), 827 (m), 770 (s), 728 (m), 678 (m), 657 (m), 597 (s), 518 (w), 465 (m), 426 (w). Mp: 145.9 °C. HPLC purity: 99.9% (t_R = 7.01 min). HRMS: calcd for $C_{17}H_{13}ClN_4O_2S$ [$M^{\bullet+}$] 372.0448, found 372.0417.

3-(2-Chlorophenyl)-6-(4-methoxybenzyl)[1,2,4]triazolo[3,4-*b*][1,3,4]thiadiazole (24). Yield: 82%. ^{1}H NMR (200 MHz, DMSO-d_6): δ [ppm] = 3.74 (s, 3H, $-OCH_3$), 4.37 (s, 2H, $-CH_2-$), 6.91−6.95 (d, 2H, ^3J = 8.72 Hz, 4″,6″-H), 7.30−7.34 (d, 2H, ^3J = 8.72 Hz, 3″,7″-H), 7.53−7.82 (m, 4H, 3′,4′,5′,6′-H). IR: 2995 (w), 1606 (w), 1585 (m), 1503 (m), 1453 (m), 1296 (w), 1238 (s), 1182 (m), 1122 (m), 1108 (m), 1027 (m), 1009 (m), 857 (m), 822 (m), 809 (m), 756 (s), 732 (m), 721 (s), 687 (w), 666 (m), 641 (m), 548 (m), 525 (m), 457 (m), 437 (m). Mp: 158.1 °C. HPLC purity: 99.9% (t_R = 7.26 min). HRMS: calcd for $C_{17}H_{13}ClN_4OS$ [$M^{\bullet+}$] 356.0498, found 356.0464.

3-(4-Fluorophenyl)-6-phenethyl[1,2, 4]triazolo[3,4-*b*][1,3,4] thiadiazole (25). Yield: 73%. ^{1}H NMR (200 MHz, DMSO-d_6): δ [ppm] = 3.12 (t, 2H, ^3J = 7.56 Hz, 1″-H), 3.45 (t, 2H, ^3J = 7.77 Hz, 2″-H), 7.18−7.54 (m, 7H, 3′,5′,4″,5″,6″,7″,8″-H), 8.12−8.31 (m, 2H, 2′, 6′-H). GC−MS (EI): 12.10 min, m/z [%] = 325.10 (22), 324.10 ([M*], 100), 121.00 (35), 91.10 (71). IR: 2980 (w), 1604 (w), 1478 (m), 1452 (s), 1221 (m), 1163 (m), 1015 (m), 970 (m), 859 (s), 814 (m), 746 (m), 719 (m), 695 (s), 632 (m), 584 (m), 521 (s), 481 (m). Mp: 165.9 °C. HPLC purity: 99.0% (t_R = 7.82 min). HRMS: calcd for $C_{17}H_{13}FN_4S$ [$M^{\bullet+}$] 324.08445, found 324.0811.

3-(2,4-Dichlorophenyl)-6-phenethyl[1,2,4]triazolo[3,4-*b*][1,3,4] thiadiazole (26). Yield: 75%. ^{1}H NMR (200 MHz, DMSO-d_6): δ [ppm] = 3.15 (t, 2H, ^3J = 7.52 Hz, 1″-H), 3.29 (t, 2H, ^3J = 7.71 Hz, 2″-H), 7.18−7.39 (m, 8H, 3′,5′,6′,4″,5″,6″,7″,8″-H). IR: 1603 (w), 1494 (w), 1470 (m), 1441 (s), 1194 (m), 1064 (w), 1016 (w), 991 (w), 977 (m), 839 (m), 750 (m), 698 (s), 687 (m), 646 (w), 567 (w), 524 (m), 493 (m). Mp: 145.5 °C. HPLC purity: 99.9% (t_R = 8.26 min). HRMS: calcd for $C_{17}H_{12}Cl_2N_4S$ [$M^{\bullet+}$] 374.01595, found 374.0142.

3-(2,4-Dichlorophenyl)-6-((4-methoxyphenoxy)methyl)[1,2,4]triazolo[3,4-*b*][1,3,4]thiadiazole (27). Yield: 73%. ^{1}H NMR (200 MHz, DMSO-d_6): δ [ppm] = 3.70 (s, 3H, $-OCH_3$), 5.49 (s, 2H, $-CH_2-$O-), 6.86−6.91 (d, 2H, ^3J = 9.22 Hz, 5″,7″-H), 7.02−7.07 (d, 2H, ^3J = 9.22 Hz, 4″,8″-H), 7.67−7.96 (m, 3H, 3′,5′,6′-H). IR: 1597 (w), 1503 (m), 1467 (m), 1238 (s), 1190 (m), 1104 (m), 1036 (m), 967 (m), 818 (s), 766 (w), 725 (w), 671 (m), 609 (m), 565 (w), 523 (m). Mp: 161.8 °C. HPLC purity: 99.9% (t_R = 7.90 min). HRMS: calcd for $C_{17}H_{12}Cl_2N_4O_2S$ [$M^{\bullet+}$] 406.0058, found 406.0074.

6-Phenethyl-3-(pyridin-4-yl)[1,2,4]triazolo[3,4-*b*][1,3,4]thiadiazole (28). Yield: 62%. ^{1}H NMR (200 MHz, DMSO-d_6): δ [ppm] = 3.06 (t, 2H, ^3J = 7.52 Hz, 1″-H), 3.39 (t, 2H, ^3J = 7.39 Hz, 2″-H), 7.08−7.41 (m, 5H, 4″,5″,6″,7″,8″-H), 7.64−7.91 (m, 4H, 2′,3′,5′,6′-H). IR: 1596 (w), 1553 (w), 1539 (w), 1496 (w), 1452 (s), 1101 (m), 1078 (w), 1051 (w), 1000 (w), 966 (m), 859 (m), 818 (s), 796 (m), 700 (m), 647 (w), 561 (m), 539 (m), 511 (w), 481 (m), 462 (m). Mp: 206.3 °C. HPLC purity: 98.5% (t_R = 6.55 min). HRMS: calcd for $C_{16}H_{13}N_5S$ [$M^{\bullet+}$] 307.0892, found 307.0906.

Acknowledgment. The research was realized with EU financial support, part of the FP6 project "Macrocept", and thanks are given to all project team members of "Macrocept". Thanks to are also given to Dr. Schachtele and Dr. Totzke (ProQinase GmbH) for testing all triazoles for their inhibition activity against a panel of protein kinases and for generating the selectivity profiles.

Supporting Information Available: Structures of purchased compounds and HRMS, HPLC, and inhibition data. This material is available free of charge via the Internet at http://pubs.acs.org.

References

(1) O'Neill, L. A. J. Targeting signal transduction as a strategy to treat inflammatory diseases. *Nat. Rev. Drug Discovery* **2006**, *5*, 549–563.
(2) Lee, J. C. ; Laydon, J. T. ; McDonnell, P. C. ; Gallagher, T. F. ; Kumar, S. ; Green, D. ; McNulty, D. ; Blumenthal, M. J. ; Heyes, J. R. A protein kinase involved in the regulation of inflammatory cytokine biosynthesis. *Nature* **1994**, *372*, 739–746.
(3) Wagner, G. ; Laufer, S. Small molecular anti-cytokine agents. *Curr. Med. Res. Rev.* **2006**, *26*, 1–62.
(4) Wrobelski, S. T. ; Doweyko, A. M. Structural comparison of p38 inhibitor−protein complexes: a review of recent p38 inhibitors unique binding interactions. *Curr. Top. Med. Chem.* **2005**, *5*, 1005–1016.
(5) Alvarez, J.; Shoichet, B. Virtual Screening in Drug Discovery; CRC Press: Boca Raton, FL, 2005.
(6) Pierce, A. C. ; Rao, G. ; Bemis, G. W. BREED: generating novel inhibitors through hybridization of known ligands. Application to CDK2, P38, and HIV Pprotease. *J. Med. Chem.* **2004**, *47*, 2768–2775.
(7) Pearlman, D. A. Evaluating the molecular mechanics Poisson−Boltzmann surface area free energy method using a congeneric series of ligands to p38 MAP kinase. *J. Med. Chem.* **2005**, *48*, 7796–7807.
(8) Zhang, Q. ; Muegge, I. Scaffold hopping through virtual screening using 2D and 3D similarity descriptors: ranking, voting, and consensus scoring. *J. Med. Chem.* **2006**, *49*, 1536–1548.
(9) Lee, H. S. ; Choi, J. ; Kufareva, I. ; Abagyan, R. ; Filikov, A. ; Yang, Y. ; Yoon, S. Optimization of high throughput virtual screening by combining shape-matching and docking methods. *J. Chem. Inf. Model.* **2008**, *48*, 489–497.
(10) Xiao, Z. ; Varma, S. ; Xiao, Y. D. ; Tropsha, A. Modeling of p38 mitogen-activated protein kinase inhibitors using the Catalyst HypoGen and k-nearest neighbor QSAR methods. *J. Mol. Graphics Modell.* **2004**, *23*, 129–138.
(11) Ottosen, E. R. ; Sorensen, M. D. ; Bjoerkling, F. ; Skak-Nielsen, T. ; Fjording, M. S. ; Aaes, H. ; Binderup, L. Synthesis and structure−activity relationship of aminobenzophenones. A novel class of p38 MAP kinase inhibitors with high antiinflammatory activity. *J. Med. Chem.* **2003**, *46*, 5651–5662.
(12) Hauser, D. R. J. ; Scior, T. ; Domeyer, D. M. ; Kammerer, B. ; Laufer, S. A. Synthesis, biological testing, and binding mode prediction of 6,9-diarylpurin-8-ones as p38 MAP kinase inhibitors. *J. Med. Chem.* **2007**, *50*, 2060–2066.
(13) Hartshorn, M. J. ; Murray, C. W. ; Cleasby, A. ; Frederickson, M. ; Tickle, I. J. ; Jhoti, H. Fragment-based lead discovery using X-ray crystallography. *J. Med. Chem.* **2005**, *48*, 403–413.
(14) Cheeseright, T. J. ; Mackey, M. D. ; Melville, J. L. ; Vinter, A. FieldScreen: virtual screening using molecular fields. Application to the DUD dataset. *J. Chem. Inf. Model.* **2008**, *48*, 2108–2117.
(15) Cheeseright, T. ; Mackey, M. ; Rose, S. ; Vinter, A. Molecular field extrema as descriptors of biological activity: definition and validation. *J. Chem. Inf. Model.* **2006**, *46*, 665–676.
(16) Low, C. M. R. ; Buck, I. M. ; Cooke, T. ; Cushnir, J. R. ; Kalindjian, S. B. ; Kotecha, A. ; Pether, M. J. ; Shankley, N. P. ; Vinter, J. G. ; Wright, L. Scaffold hopping with molecular field points: identification of a cholecystokinin-2 (CCK2) receptor pharmacophore and its use in the design of a prototypical series of pyrrole- and imidazole-based CCK2 antagonists. *J. Med. Chem.* **2005**, *48*, 6790–6802.
(17) Stelmach, J. E. ; Liu, L. ; Patel, S. B. ; Pivnichny, J. V. ; Scapin, G. ; Singh, S. ; Hop, C. E. C. A. ; Wang, Z. ; Strauss, J. R. ; Cameron, P. M. ; Nichols, E. A. ; O'Keefe, S. J. ; O'Neill, E. A. ; Schmatz, D. M. ; Schwartz, C. D. ; Thompson, C. M. ; Zaller, D. M. ; Doherty, J. B. Design and synthesis of potent, orally bioavailable dihydroquinazolinone inhibitors of p38 MAP kinase. *Bioorg. Med. Chem. Lett.* **2003**, *13*, 277–280.
(18) Laufer, S. ; Thuma, S. ; Peifer, C. ; Greim, C. ; Herweh, Y. ; Albrecht, A. ; Dehner, F. An immunosorbent, nonradioactive p38 MAP kinase assay comparable to standard radioactive liquid-phase assays. *Anal. Biochem.* **2005**, *344*, 135–137.
(19) Carhart, R. E. ; Smith, D. H. ; Venkataraghavan, R. Atom pairs as molecular features in structure−activity studies: definition and applications. *J. Chem. Inf. Comput. Sci.* **1985**, *25*, 64–73.
(20) Lehmann, F. ; Holm, M. ; Laufer, S. Three-component combinatorial synthesis of novel dihydropyrano[2,3-*c*]pyrazoles. *J. Comb. Chem.* **2008**, *10*, 364–367.
(21) Malhotra, S. ; Manher, V. ; Chadha, V. K. Bridgehead nitrogen heterocycles: syntheses of 3,6-disubstituted-*s*-triazolo[3,4-*b*][1,3,4] thiadiazoles, and related systems. *Indian J. Heterocycl. Chem.* **2003**, *12*, 257–262.

(22) Invidiata, F. P. ; Furno, G. ; Lampronti, I. ; Simoni, D. 1,2,4-Triazoles. Improved synthesis of 5-substituted 4-amino-3-mercapto-(4*H*)-1,2,4-triazoles and a facile route to 3,6-disubstituted 1,2,4-triazolo[3,4-*b*][1,3,4]thiadiazoles. *J. Heterocycl. Chem.* **1997**, *34*, 1255–1258.
(23) Reid, J. R. ; Heindel, N. D. Improved syntheses of 5-substituted-4-amino-3-mercapto-(4*H*)-1,2,4-triazoles. *J. Heterocycl. Chem.* **1976**, *13*, 925–926.
(24) http://www.accelrys.com/ (accessed Oct 3, 2008).
(25) http://www.cresset-bmd.com/xedex.shtml (accessed Oct 3, 2008).
(26) Brown, R. D. ; Martin, Y. C. Use of structure−activity data to compare structure-based clustering methods and descriptors for use in compound selection. *J. Chem. Inf. Comput. Sci.* **1996**, *36*, 572–584.
(27) Sheridan, R. P. ; Hunt, P. ; Culberson, J. C. Molecular transformations as a way of finding and exploiting consistent local QSAR. *J. Chem. Inf. Model.* **2006**, *46*, 180–192.
(28) http://www.cresset-bmd.com/fieldalign.shtml (accessed Oct 3, 2008).